Cellular and Molecular Life Sciences (2025) 82:128
https://doi.org/10.1007/s00018-025-05574-3

ORIGINAL ARTICLE

The HBV large envelope protein initiates virion assembly by recruiting capsids at membrane rich domains related to late endosome

Florian Seigneuret[1] · Sébastien Eymieux[1,2] · Vanessa Sarabia-Vega[1] · Roxane Lemoine[3] · Julien Burlaud-Gaillard[2] · Pierre Raynal[2] · Christophe Hourioux[1,2] · Camille Sureau[1] · Philippe Roingeard[1,2] · Hugues de Rocquigny[1]

Received: 30 April 2024 / Revised: 6 December 2024 / Accepted: 2 January 2025

Abstract

A crucial step of HBV (Hepatitis B Virus) virion morphogenesis is the envelopment of the nucleocapsid by the viral envelope proteins, which is triggered by an interaction between the HBV core protein and the large HBV envelope protein. To document this protein–protein interaction, we co-expressed core and large HBV envelope (LHBs) in Huh-7 cells and subjected the cells to microscopy examination by Fluorescence Resonance Energy Transfer (FRET) and Transmission Electron Microscopy (TEM). Our results show that the sole expression of the core protein leads to assembly of capsids that remain individually isolated within the whole cell, but particularly within the nucleus. In the presence of LHBs, capsids were observed as large clusters in a membrane rich region peripheral to the nucleus. In this context, core-LHBs complex co-localize with markers of the late endosome/multivesicular bodies, this co-localization being driven by LHBs. These results thus show that LHBs binds to the core proteins when preassembled into capsid, at membranes of the late endosome, where the inner capsid and the outer envelope meet to assemble a virion.

Keywords HBV · Capsid · Core · Envelope · HBc · Viral assembly · Late endosomes · Fluorescent microscopy · Electron microscopy

Abbreviations

HBV	Hepatitis B virus
HBc	Hepatitis B core
FRET	Fluorescence resonance energy transfer
FLIM	Fluorescence lifetime imaging microscopy
TEM	Transmission electron microscopy
LHBs	Large HBV envelope protein
SHBs	Small envelop protein

Introduction

Hepatitis B virus (HBV) chronic infections affect more than 250 million individuals worldwide and lead to the death of up to one million individuals per year from liver diseases such as, cirrhosis, and hepatocellular carcinoma. The HBV virion is 42 nm in diameter, consisting of (i) an inner nucleocapsid (NC) that contains partially double-stranded relaxed circular HBV DNA (rcDNA) covalently linked to the viral polymerase (P) and (ii) an outer envelope made of lipids and three types of HBV- encoded envelope proteins. The latter bear the HBV surface antigen (HBs) and are referred to the large (LHBs), middle (MHBs) and small (SHBs) proteins [1]. SHBs, a 226 aas in length protein can self-assemble to form empty subviral particles (SVPs) [2, 3]. MHBs protein is larger than SHBs by 55 aas (the pre-S2 domain); it is included in the envelope of HBV virions and SVPs but is dispensable for viral replication and infection [4–6]. LHBs contains an additional N-terminal pre-S1 domain that is essential at two steps of the HBV life cycle: (i) assembly and release of enveloped HBV virion and (ii) entry into human hepatocytes upon binding to the sodium taurocholate

✉ Hugues de Rocquigny
hderocquigny@univ-tours.fr

[1] INSERM U1259 MAVIVH, Université de Tours and CHRU de Tours, 10 boulevard Tonnellé, BP 3223, 37032 Tours Cedex 1, France

[2] Plate-Forme IBiSA des Microscopies, PPF ASB, Université de Tours and CHRU de Tours, 10 boulevard Tonnellé, BP 3223, 37032 Tours Cedex 1, France

[3] Département Cytométrie et Single-Cell Immunobiologie, Plateforme Scientifique et Technique - Analyse des Systèmes Biologiques (PST-ASB), Université de Tours, 10 Boulevard Tonnellé, 37032 Tours Cedex 1, France

Published online: 24 March 2025

co-transporting polypeptide (NTCP), the cell surface receptor for HBV [7–11].

The formation of HBV NC is initiated by an interaction between pre-genomic RNA (pgRNA), polymerase and core proteins [12]. Within the NC, pgRNA is reverse-transcribed into rcDNA [13, 14] and NC envelopment with surface glycoproteins was reported to use the autophagy and the endosomal sorting complexes required for transport (ESCRT) machineries to traffic from ER to multivesicular bodies (MVBs) [1, 15–21]. It has also been reported that the HBV envelope proteins are ubiquitinated to allow for a E3 ubiquitin-protein ligase (NEDD4)-dependent secretion of particles through MVBs using the γ2-adaptin [22, 23].

However, the mechanism of HBV virion envelopment and its precise intracellular location remain elusive [13, 24]. It is important to note that in addition to DNA-containing virions, an excess of empty virions, i.e. virions containing a genome-free capsid, are assembled [25], which are indistinguishable by size and shape from DNA-containing virions [22, 26, 27].

In this study, we aimed at tracing the intracellular path of core and LHBs proteins to identify the cellular compartment in which they meet to promote HBV virion formation [28–32]. In vitro studies based on synthetic peptides have shown evidence for a direct interaction between the two partners [33, 34], whereas in cells co-expressing core and LHBs, there was evidence for LHBs being used as a platform for the clustering of core and SHBs [35]. In this study, we co-expressed core and LHBs in Huh-7 cells. Using both quantitative fluorescent microscopy and transmission electron microscopy techniques we could document a direct core-LHBs interaction localized at the periphery of the nucleus. Our results show that in the absence of LHBs, core proteins, assemble into capsids that remain individually dispersed in both nucleus and cytoplasm. In contrast, when LHBs is co-expressed with core, large number of capsids but not of core accumulate with LHBs in membrane rich domains. Interestingly, capsid localization and envelopment in neutral late endosomes/MVBs is dependent on LHBs.

Materials and methods

Plasmids

LHBs expression vector was described previously [35]. Derivative vectors for expression of eGFP-LHBs or mCherry-LHBs were constructed by inserting the eGFP or mCherry DNA coding sequence at the 5'-end of LHBs DNA coding sequence. The LHBs deleted from the Matrice Binding Domain (ΔMBD) mutant was generated by overlap PCR mutagenesis. HBV core expression vectors was described previously [36]. All plasmid used for transfection were subjected to DNA sequencing.

Cell culture and transfection

Huh-7 cells were obtained from ATCC (Manassas, VA, USA). These cells are derived from hepatocellular carcinomas [37] and permissive for HBV replication [38]. Cells were grown at 37 °C/5% CO_2 and maintained in Williams' Medium supplemented with 10% bovine serum (Gibco, France) and 0.1% gentamicin (Invitrogen Corporation Pontoise, France). Transfections were carried out with JetPEI™ (Ozyme, France) following the supplier's recommendation. All transfection experiments were normalized for DNA concentration using the empty pcDNA3 plasmid (Invitrogen). For immunofluorescence (IF) or Fluorescence Lifetime Imaging (FLIM) experiments, transfections were performed with 0.3 or 1 µg of total plasmid DNA per well of a 12-well plate containing glass coverslips or 8-well Ibidi plates, respectively. For TEM, transfection was performed with 10 µg of plasmid DNA per 75 cm^2 flask.

Immunoblot analysis

Seventy-two hours post-transfection, Huh-7 cells were washed with Dulbecco phosphate buffered saline (DPBS) and total cell extracts were obtained by lysing the cells directly with ice-cold RIPA buffer (25 mM Tris–HCl pH 7.6, 150 mM NaCl, 1% NP-40, 1% sodium deoxycholate, 0.1% sodium dodecyl sulfate (SDS)) supplemented with complete anti-protease cocktail (Thermo Fisher). The lysate was subsequently subjected to centrifugation (10,000 rpm, 4 °C, 10 min.) and the supernatant analyzed for protein concentration using a Pierce BCA Protein Assay Kit (Thermo Fisher Scientific). Forty µg of total protein were diluted in reducing 6X Laemmli SDS sample buffer (Thermo Fisher), heat denatured and subjected to SDS-PAGE (TGX 12% miniprotean gel TGX, Bio-Rad). After electrophoresis, proteins were transferred onto a Western blot PVDF membrane (Bio-Rad). The membrane was blocked with 5% non-fat milk in Tris-buffered saline (TBS)/0.3% Tween20 (TBST) for 1 h at 37 °C. For β-Actin antibody the blocking solution was TBST and 3% Bovine serum albumin-BSA. The subsequent primary and secondary incubations used the same conditions as the blocking. The primary and secondary antibodies were incubated on the blot at room temperature (RT) for 1 h or at 4 °C overnight, and for 1 h at RT respectively. The blot was developed using PierceTM ECL detection system (Thermo Fisher) according to the manufacturer's protocol. Chemiluminescence was detected on an Imagequant LAS500 apparatus (GE Healthcare). The following primary antibodies were used: (i) a human anti-HBc polyclonal antibody at a 1:2000 dilution as described [39], (ii) a mouse anti-HBs monoclonal

antibody (1:2000, 70HG15, Fitzgerald), (iii) a rabbit polyclonal anti-GFP antibody (1:4000, ab6556, Abcam), (iv) a mouse Monoclonal anti-mCherry antibody [1C51] (1:4000, ab125096, Abcam), (v) and a rabbit polyclonal β-beta Actin antibody (1:4000, ab8227, Abcam). Goat anti-rabbit IgG H&L (HRP) (1:6000, ab6721, Abcam), donkey anti-goat IgG H&L (HRP) (1:8000, ab6885, Abcam), goat anti-human IgG Fc (HRP) (1:6000, ab97225, Abcam) and goat anti-mouse IgG H&L (HRP) (1:8000, ab205719, Abcam) secondary antibodies were used.

Confocal microscopy

Huh-7 cells grown overnight on glass coverslips were fixed in 4% paraformaldehyde for 10 min. and permeabilized and blocked with 0.2% Triton × 100, 0.4% BSA, in PBS for 30 min. Cells were incubated overnight with primary antibodies diluted in 0.4% BSA at 4 °C, followed by incubation with the appropriate secondary antibody for 1 h at room temperature. Nuclei were stained with DAPI (Sigma) prior to mounting of coverslips on slides using Fluoromount-G (Thermo Fisher).

The primary antibodies used for the endosomal markers were: mouse anti-Calreticulin [TO-11] (C7492, Sigma-Aldrich), rabbit anti- Protein Disulfide Isomerase (PDI) [DL-11] (P7122, Sigma-Aldrich), mouse anti-Rab5A antibody—Early Endosome Marker (ab18211, Abcam), mouse anti-Rab9 [Mab9] (ab2810, Abcam), mouse anti-CD81 clone 5A6 [40], anti-Rab7 [Rab7-117] – Late Endosome Marker (ab50533, Abcam), mouse anti-HA tag antibody [HA.C5] (ab18181, Abcam), mouse anti-LAMP1 antibody [H4A3] (ab25630, Abcam), mouse anti-LAMP-2 [H4B4] (Santa Cruz Biotech., H4B4), human anti-HBc polyclonal antibody [35], goat anti-HBsAg antibody (70-HG15; Fitzgerald industries) or rabbit polyclonal anti-preS1 (R271) [41]. For LC3, Lamp1 and TSG101, Huh-7 cells were co-transfected with HBV core and LHBs expressing vectors, together with the pLC3-Aquamarine [42], Lamp1-mTurquoise2 (Addgene #98,828) or pHA-TSG101 [43] plasmids DNA, respectively.

The following secondary antibodies were used: goat anti-mouse IgG (H + L) Alexa Fluor 488 (Invitrogen); donkey anti-rabbit IgG (H + L) Alexa Fluor 488 (Invitrogen), donkey anti-human IgG (H + L) DyLight 594 (Invitrogen), donkey anti-goat IgG (H + L) Alexa Fluor 647 (Invitrogen), donkey anti-rabbit IgG (H + L) Alexa Fluor 647 (Invitrogen).

Visualization of acidic organelles was performed by life-imaging staining with 50 nM green LysoTracker DND-26 (Invitrogen). After 72 h, cells transfected with core/mCherry-core (90/10) plasmid combination, or with LHBs/mCherry-LHBs (95/5) plasmid combination, were washed and incubated with DAPI and 1:10,000 green LysoTracker in Leibovitz's L-15 medium (Thermo Fisher Scientific), at 37 °C for 30 min.

Fluorescence confocal images were taken using a confocal microscope LEICA SP8 gSTED equipped with 60 × PL APO 1.30 CS2 Oil and laser diode at 405 nm for DAPI, argon laser at 488 nm for Alexa 488 and white laser at 594 nm for Alexa 594, or at 647 nm for Alexa 647. DNA was stained with DAPI (2-(4-Amidinophenyl)−6-indolecarbamidine dihydrochloride, Sigma) (1 mg/ml, 1:10,000).

Image analysis

All images were acquired with identical channel settings for each endosomal/lysosomal marker. The Pearson's correlation coefficient (PCC) was calculated for 15–25 cells depending on the experiment, from at least two independent experiments using the JACoP v2.0 plugin for ImageJ. For quantification of co-localization the LHBs or core regions were outlined in the magenta or yellow channel respectively. The regions of interest (ROI) selected were used in each channel to subtract background noise for each image. The mean PCC was represented as bars, each analyzed cell as scatter dots and the standard deviations as error bars.

Cell sorting by FACS

Huh-7 cells in 75-cm^2 flasks were transfected with 16 µg of plasmid DNA including 7.2 µg of wt LHBs plasmid, 0.8 µg LHBs-eGFP plasmid and 8 µg core expressing plasmid. A gating was done using the BD FACS ChorusTM software (BD Biosciences). Cell sorting was performed with a 100 µm nozzle and sorted directly in tubes containing cell culture medium. After establishing the basic gating parameters, $3. \times 10^5$ to 1×10^6 GFP-positive cells for each population of interest, were sorted at a speed of 6000 cells/s.

Immuno-electron microscopy according to the Tokuyasu method

Huh-7 cells transfected for expression of LHBs and core proteins, or derivatives were harvested at 72 h post transfection. Cells were sorted as described above and fixed for 1 h at 4 °C with 4% paraformaldehyde, 0.05% glutaraldehyde in PBS. Cells were washed twice with PBS and embedded in 12% gelatin, then infused with 2.3 M sucrose overnight at 4 °C before ultrathin cryo-sectioning on a Leica FC7 cryo-ultramicrotome at −100 °C. Sections of 80 nm thickness were retrieved in a mix of 2% methylcellulose supplemented with 2.3 M sucrose (1:1) and deposited onto formvar/carbon-coated nickel grids.

Immunogold labeling on ultrathin cryo-sections

Sections were incubated at 37 °C to remove gelatin, then saturated with BSA (Aurion, Wageningen, the Netherlands) for

30 min at room temperature. After 3 washes in PBS, 0.1% BSA, sections were incubated in PBS, 0.1% BSA containing a 1:100 dilution of human anti-HBc polyclonal antibody, or a 1:100 dilution of rabbit anti-preS1 R254 [41], or 1:200 dilution of rabbit anti-GFP monoclonal antibody (Abcam, ab6556). After six washes in PBS, 0.1% BSA, the grids were incubated in PBS, 0.1% BSA containing a 1:30 dilution of the cognate gold-conjugated antibody (Aurion, Wageningen, the Netherlands). The grids were finally washed six times in PBS, 0.1% BSA and three times in distilled water. Contrast staining was achieved by incubating the grids in a 2% uranyl acetate, 2% methylcellulose mixture (1:10) for 10 min at room temperature. The sections were observed using a transmission with a JEOL JEM-1011 (Tokyo, Japan) transmission electron microscope operated at 100 kV and equipped with an Ametek-GATAN RIO9 CMOS camera.

Transmission electron microscopy

Seventy-two hours post transfection with LHBs and eGFP-LHBs expressing plasmid DNA (95/5), cells were sorted and fixed by incubation for 24 h in 4% paraformaldehyde and 1% glutaraldehyde (Sigma, St. Louis, MO) in 0.1 M phosphate buffer (pH7.2). Fixed cells were washed with PBS and incubated with 2% osmium tetroxide (Agar Scientific, Stansted, UK) for 1 h. Fixed cells were then fully dehydrated in increasing concentration of ethanol (70%, 90% and 100%) and then propylene oxide (100%). Fixed cells were then impregnated with a 1:1 mixture of propylene oxide/Epon resin (Sigma) and incubated overnight in pure resin. Cells were then embedded in Epon resin (Sigma) and left to polymerize for 48 h at 60 °C. Ultrathin Sects. (80 nm) were cut with an EM UC7 ultramicrotome (Leica Microsystems, Wetzlar, Germany). Contrast staining was performed with 2% uranyl acetate (Agar Scientific) and 5% lead citrate (Sigma), and the samples were then observed with a JEOL JEM-1011 (Tokyo, Japan) transmission electron microscope operated at 100 kV and equipped with an Ametek-GATAN RIO9 CMOS camera.

Fluorescence lifetime imaging microscopy (FLIM)

Huh-7 cells seeded in micro-slide 8-well Ibiditreat plate were transfected with a mixture plasmid DNA coding for core, core-eGFP (ratio 0.7/0.3) and mCherry-LHBs. The same conditions were used for core or LHBs derivatives. Post transfection, cells were incubated for 72 h then incubated in phenol red-free Leibovitz's L-15 medium (Thermo Fisher Scientific) supplemented with 5% fetal bovine serum and 0.1% of gentamicin [36]. Live cells were then observed by FLIM in thermostatic chamber at 37 °C.

Images were acquired with a Leica TCS SP8 confocal system, equipped with a pulsed 470–670 nm White Light Laser and Hybrid Detectors capable of photon counting and fluorescence lifetime imaging. FLIM acquisitions are performed in TCSPC mode (time-correlated single photon counting) thanks to the integrated Leica FALCON module (FAst Lifetime CONtrast). FALCON performs high speed FLIM acquisitions up to 1 detected photon per pulse (80 Mcts) with < 1.5 ns dead time and 97 ps time resolution, and FLIM data analysis using decay fitting.

The FRET efficiency (E) was calculated according to:

$$E = 1 - \frac{\tau DA}{\tau D} \quad (1)$$

where τDA is the lifetime of the donor in the presence of the acceptor and τD is the lifetime of the donor in the absence of the acceptor.

Results

Imaging core-LHBs interaction by FLIM

Recently, we, among others, documented the intracellular co-localization of LHBs and core proteins in HBV-permissive cells and concluded that LHBs would serve as a platform for HBV virion assembly by recruiting core and SHBs proteins [35, 44, 45]. However, evidence for a direct protein–protein interaction in the cellular environment is missing. Here we used a FRET assay to visualize in cell the core-LHBs interaction when these two partners are co-expressed using a set of tagged proteins: core-eGFP, eGFP-LHBs or mCherry-LHBs as a tracer (Fig. 1A, C). Insertion of eGFP between residues 78 and 80 of the core protein was shown permissive for capsid assembly (Fig. 1B) [36, 46]. Note that in this scheme only one eGFP or mCherry was drawn at the tips of each dimer to illustrate that cells are co-transfected with plasmids expressing both labelled and unlabelled core proteins [36]. As shown in Fig. 1E–G, the results of a western blot analysis revealed that each chimeric protein was detected at the expected molecular weight. Both eGFP-LHBs and mCherry-LHBs lack the N-terminal myristate, a post-translational modification essential for viral entry but dispensable for HBV morphogenesis [47, 48].

The eGFP-mCherry fusion protein was used here as a FRET-positive control (not shown) [49, 50]. FRET between eGFP and mCherry occurs only when the two proteins are less than 5–7 nm apart, a distance assumed to indicate a direct protein–protein interaction [51, 52]. FRET is measured by calculating the lifetime (τ) of eGFP (FLIM), an intrinsic parameter of the chromophore, which is independent of its concentration. However, the eGFP lifetime value is highly sensitive to its environment and decreases during FRET. It is calculated pixel-by-pixel on a cell expressing the eGFP partner only, and it is compared

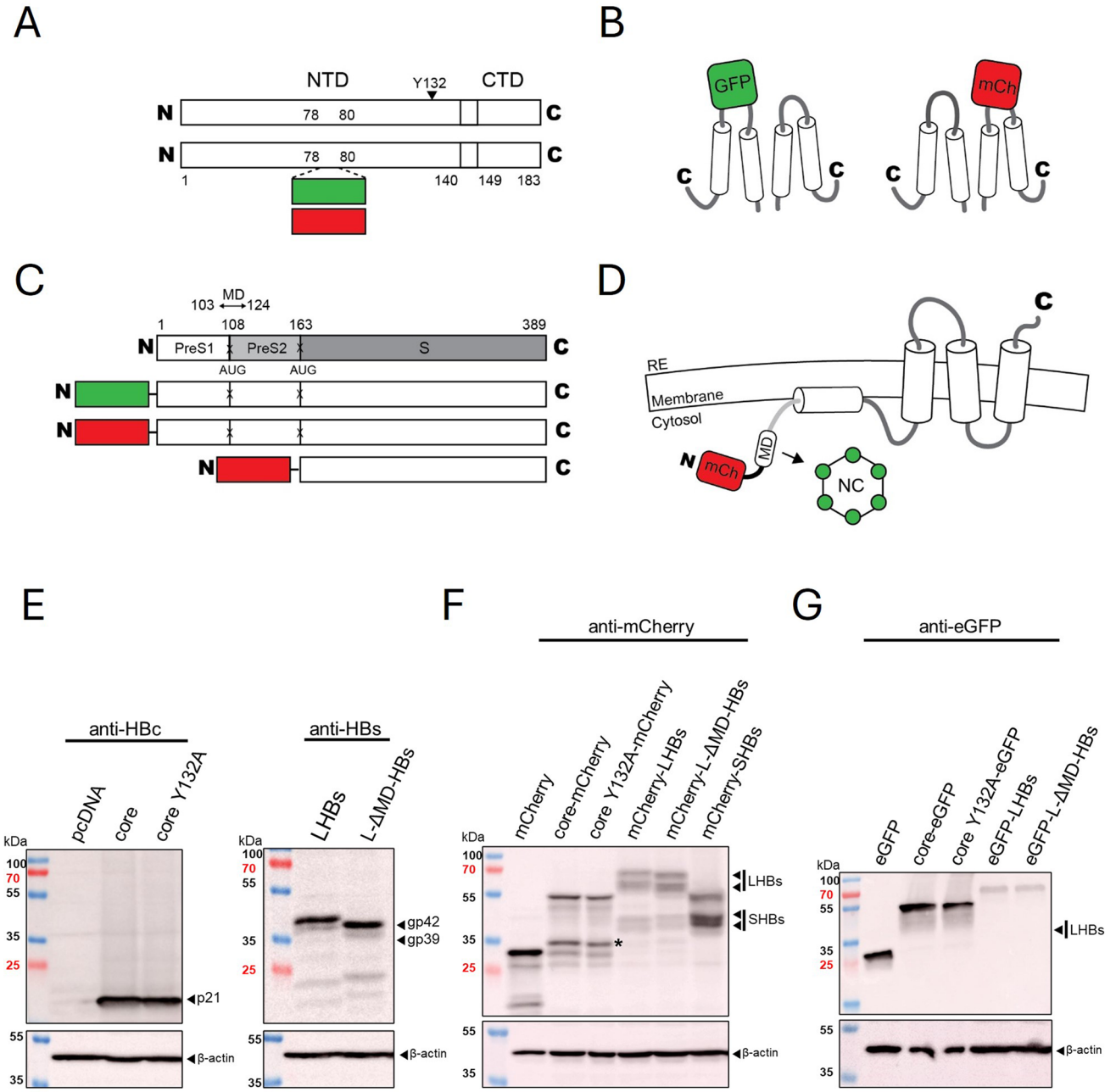

Fig. 1 HBV core and HBV LHBs constructs. A: Core-NTD, linker (140–149) and CTD are depicted. eGFP or mCherry polypeptides have been inserted between positions 78 and 80. Y132A mutant is localized with a dark arrow. B: Diagram of a core dimer with an eGFP or mCherry positioned at the top of helix 3. C: Schematic representation of LHBs protein with preS1, preS2 and S domains. X indicates that AUG codons were changed to ACG to prevent translation of the M- and SHBs proteins. The eGFP and mCherry proteins were placed at the N-terminus of LHBs or SHBs. MD is the Matrix Domain that corresponds to the residues 103–124. D: Scheme of the interaction between the nucleocapsid labelled with eGFP and the MD domain of the i-PreS topology of LHBs labelled with mCherry. E: Western blot analysis of core, coreY132A, LHBs and L-ΔMD-HBs using anti-HBc (left panel) or anti-HBs (right panel). β–actin was used as control. F: Western blot analysis of mCherry, core-mCherry and mCherry-LHBs derivatives using anti-mCherry antibody. G: Western blot analysis of eGFP, core-eGFP and eGFP-LHBs derivatives using an anti-eGFP antibody. * corresponds to a partial hydrolysis of core-mCherry and core-mCherry derivatives as previously observed in [36]

to the lifetime calculated on a cell expressing both eGFP and mCherry partners. An image is then reconstructed using an arbitrary color scale so that the color differences provide a spatial representation of the interaction between the two partners.

Figure 2A, B shows representative images of alive cells expressing core/core-eGFP + mCherry (upper row) or core/core-eGFP + mCherry-LHBs (lower row). Images were obtained by confocal microscopy (panel A), and by lifetime measurements (panel B). In cell co-expressing core and core-eGFP, together with mCherry, core proteins accumulate in the nucleus (Fig. 2, upper row, image a) whereas mCherry diffuses into the entire cell (Fig. 2A, image b). This led to a yellow staining in the nucleus when the channels were superimposed (Fig. 2A, image c). By FLIM, the nuclear yellow staining (Fig. 2B, image d) corresponds to an average τ value equal to 1.94 ± 0.1 ns (orange arrow on the arbitrary color scale), equivalent to that of free core-eGFP, since eGFP does not interact with mCherry. It should be noted that the eGFP lifetime is usually at 2.3–2.4 ns [53], however we previously observed that core-eGFP had a shorter-than-expected lifetime, probably as a result to its involvement into capsid assembly [36].

In cells co-expressing core + core-eGFP + mCherry-LHBs (Fig. 2A, second row), core proteins accumulated at the nuclear periphery (Fig. 2A, image e), and co-localized with large clusters of LHBs (Fig. 2A, images f and g). An LHBs-mediated delocalization of core at the rim of the nucleus was previously reported [35, 44, 54]. The average core-eGFP lifetime for the whole cell was 1.68 ± 0.07 ns (Fig. 2B, image h) for a FRET efficiency of $14.69 \pm 3.4\%$ (Fig. 2D). However, the spatial distribution of this lifetime was heterogeneous throughout the cell. Indeed, a yellowish color is observed in the nuclei of the two images d and h. This color corresponds to a long lifetime ($\tau_{nu} = 1.9$–2 ns, yellow arrow on the scale) of free core-eGFP proteins. On the other hand, a bluish color is located at the periphery of the nucleus of cells co-expressing the two partners (image h) and corresponds to a short lifetime ($\tau_{cyt} = 1.3$–1.5 ns, turquoise arrow on the scale) of core-eGFP proteins interacting with mCherry-LHBs. This observation is in support of a direct interaction between the core and LHBs, in the cytoplasm, at the periphery of the nucleus, while the free core protein remained localized within the nucleus.

To further investigate an intracellular interaction between LHBs and core by FRET, we substituted (i) envelopment deficient mCherry-SHBs or mCherry-L-ΔMD-HBs [28] to mCherry-LHBs, and (ii) a capsid assembly deficient coreY132A to wt core [55, 56]. When transfected cells were observed by confocal microscopy (not shown) and FLIM, nuclei appeared as yellow corresponding to long lifetime (Fig. 2C, images b, c and d) and, consequently, to a low FRET efficiency at around 5% (Fig. 2D). These results are in support of (i) SHBs not interacting with core in absence of LHBs [35] and (ii) the MD domain of LHBs being required for interacting with core [28]. The lack of FLIM observed when coreY132A was substituted to wt core strongly indicates that LHBs interacts with core in a preassembled capsid. Note that the deletion of MD has no impact on LHBs oligomerization [57] (Fig. S1) and that capsid-assembly deficient coreY132A poorly oligomerizes (Fig. S2) [36, 55, 56]. Our results also show that co-expression of the eGFP- or mCherry-fusion proteins with their wt counterpart does not prevent interaction between capsid and LHBs.

HBV capsids and LHBs co-localize in large clusters

Because TEM can reach nanometric resolution, it allows for the observation of cell ultrastructure and viral particles. To go further in the characterization of core-LHBs complex, immuno-TEM was used following the Tokuyasu method [58]. In this method, the sample is fixed under mild conditions in the presence of glutaraldehyde and frozen to obtain ultrathin sectioning in a sucrose solution as cryoprotectant to avoid ice crystal formation. Finally, the sample is processed in aqueous environment that preserves the ultrastructure of the protein accessible to antibodies. In this approach cells were transfected with DNA vectors coding for (i) core/core-GFP (90/10) (Fig. 3a), (ii) LHBs/eGFP-LHBs (95/5) (Fig. 3b), and (iii) core/LHBs/eGFP-LHBs (50/45/5) (Fig. 3c). Post-transfection, cells were sorted by FACS for eGFP expression, and selected cells were then treated for immuno-TEM using anti-HBc or anti-preS1 antibodies.

In cells expressing core only, we observed that core-specific 6 nm-gold beads surrounded spherical and electron dense material corresponding to native HBV capsid (Fig. 3a and enlargement, yellow arrows). The distance observed between capsid and the gold beads was compatible to the size of the primary-secondary antibody pair. Note that capsids (identified by their apparent icosahedral shape) were not always decorated with gold beads. We interpret this as a lack of antibody accessibility, as is often the case with this type of technique.

In agreement with the fluorescent microscopy images (Fig. 2), capsids were mainly observed in cell nucleus (Fig. 3a), but occasionally in the cytoplasm (Fig. S3). But whatever their intracellular localization, capsids were always evenly dispersed and distanced from each other. Interestingly, we could not document any proximity between capsids and cell membranes. This implies that, unlike assembly

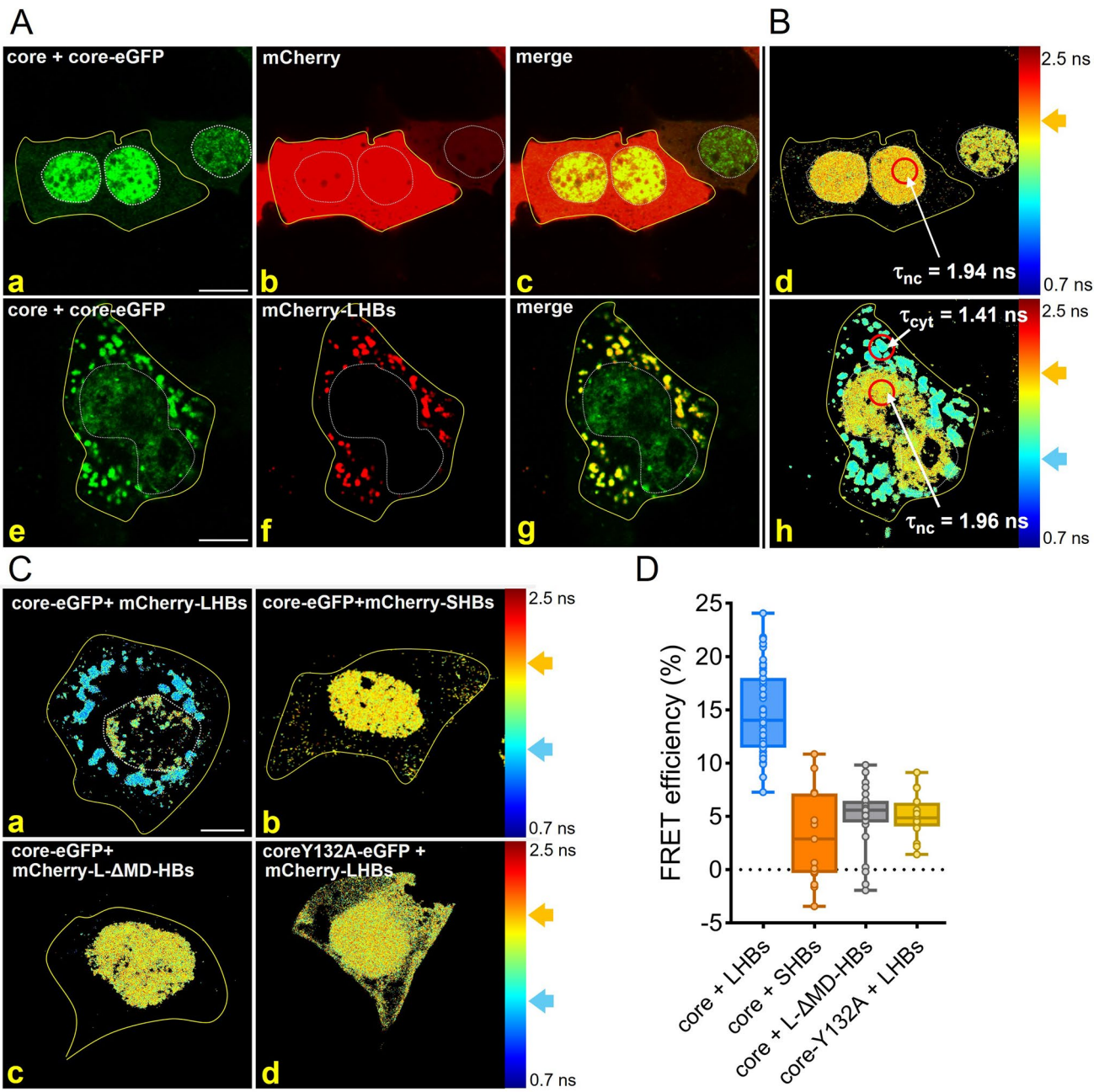

Fig. 2 Imaging HBV LHBs and core interaction by FRET. A and B: Huh-7 cells were transfected with a mix of plasmids expressing core, core-eGFP- (70/30) and either mCherry (row 1, images a-d) or mCherry-LHBs (row 2, images e–h). 72 h post transfection, Williams medium was substituted for Leibovitz's L-15 medium supplemented with 5% fetal bovine serum and placed at 37 °C in thermostatic chamber. Live cells were observed simultaneously by confocal microscopy (panel A) and FLIM (panel B). The fluorescence lifetime τ was measured pixel per pixel and converted into color using a color scale ranging from blue (0.7 ns = short fluorescence lifetime) to red (2.5 ns = long fluorescence lifetime). The red circles in the nucleus or in the cytoplasm of images d and h show a heterogeneous spatial distribution of lifetime (τ_{nc} for τ nucleus and τ_{cyt} for τ cytoplasm). C: Huh-7 cells were transfected with a mix of plasmids expressing core, core-eGFP (70/30) and either mCherry-LHBs (image a) or mCherry-SHBs (image b) or mCherry-L-ΔMD-HBs (image c). For image d, Huh-7 cells were transfected with plasmid expressing mCherry-LHBs and a mix of plasmids expressing coreY132A and coreY132A-eGFP (70/30). FLIM measurements and image analysis were then carried out as for Fig. 2B using the same color scale. A scale bar in white is reported represents 10 µm. White dots delineate the cell nucleus and yellow lines the cell membrane. D: Histograms of FRET efficiency for various LHBs or core derivatives. Box and whiskers plots of the FRET efficiency (E) was determined at 72 h post transfection. FRET efficiency E was calculated using the Eq. (1) where τ_{DA} is the lifetime of the donor in the presence of the acceptor and τ_D is the lifetime of the donor in the absence of the acceptor

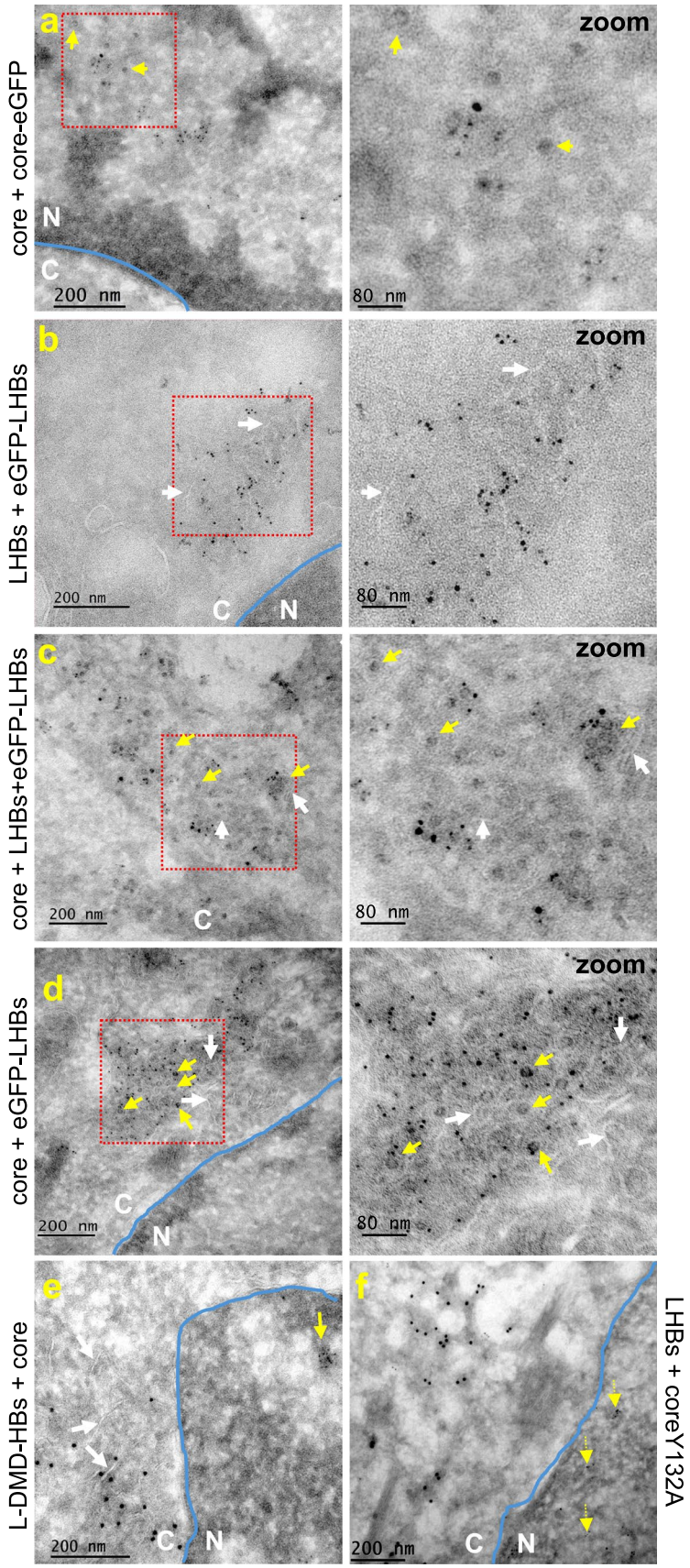

Fig. 3 Immuno-TEM of core and LHBs by the Tokuyasu method. Huh-7 were transfected with a mixture of plasmids expressing (a) core and core-eGFP (90/10); (b) LHBs and eGFP-LHBs (95/5), (c) core, LHBs and eGFP-LHBs (50/45/5); (d) core, LHBs and eGFP-LHBs (50/45/5); (e) core, L-ΔMD-HBs and eGFP-L-ΔMD-HBs (50/45/5) or (f) coreY132A, LHBs and eGFP-LHBs (50/45/5) for 72 h. Transfected cells were sorted by monitoring eGFP expression and fixed prior to gelatin inclusion. Ultrathin sections were cut (80 nm) and incubated with human anti-HBc (images a, c, e and f), rabbit anti-PreS1 (images b, c, e and f), rabbit anti-eGFP (image d), and then with a 6-nm gold-conjugated anti-human antibody (image a, e and f) or a 10-nm gold-conjugated anti-human antibody (image c) or a 6-nm gold conjugated anti-rabbit antibody (images b, c and d) or a 10-nm gold conjugated anti-rabbit antibody (images e and f). Scale is reported at the bottom left. Some capsids are indicated by yellow arrows, core proteins in the nucleus are indicated by dashed yellow arrows and membrane rich domains with white arrows. Nucleus are delimited by a blue line

of HIV Gag protein [59], HBV core assembly into capsid would not depend on membrane association.

Using anti-preS1 primary antibody and secondary antibody bound to 6 nm bead for immuno-TEM of cells expressing LHBs and eGFP-LHBs, the latter were always detected in large clusters, exclusively in the cytoplasm at the periphery of the nucleus (Fig. 3b and enlargement). Furthermore, clusters of LHBs proteins co-localized with convoluted membranes (designed by white arrows in Fig. 3b).

When immuno-TEM was performed on cells expressing core + LHBs + eGFP-LHBs, capsids were identified by their apparent icosahedral structure and by anti-core specific followed by anti-human bound to 10 nm beads, while envelope proteins were detected with anti-PreS1 and a 6 nm beads-labeled secondary antibodies (Fig. 3c). Numerous capsids (yellow arrows) appeared as clusters, whereas LHBs remained associated to membrane rich region (white arrows). Our interpretation of the data is that the encounter between envelope proteins and capsid is mediated by membrane associated LHBs. As shown in Fig. 3a, capsids remain individually dispersed in the absence of LHBs, whereas in its presence, they cluster with LHBs (Fig. 3c).

To corroborate that the observed capsids were equally associated with LHBs and eGFP-LHBs, we performed immuno-TEM only with an anti-eGFP antibody and a secondary antibody bound to 6 nm beads, capsid being clearly identified by their icosahedral structure. As shown in Fig. 3d, capsid clusters (yellow arrows) associate with LHBs (gold beads) in a convoluted membrane environment (white arrows) close to the nucleus. All together, these data are in support of LHBs condensing capsids at intracellular membranes.

In support of this interpretation, we showed that L-ΔMD-HBs protein could also cluster (Fig. 3e) in a membrane-rich region (white arrows) close to the nucleus but, as expected, co-expressed capsids remained dispersed within the nucleus (yellow arrow). This agrees with the absence of FRET efficiency reported above (Fig. 2), and it confirms the essential role of LHBs MD in LHBs-induced capsid recruitment and virion assembly [32, 60, 61].

At least, when cells co-expressing wt-LHBs and coreY132A proteins were subjected to immuno TEM, the LHBs-specific 10 nm beads clustered in the cytoplasm (Fig. 3f, white arrows), but core-specific 6 nm beads remained dispersed in the nucleus in the absence of assembled capsids (yellow dotted arrow) with no evidence of LHBs-associated clusters. This emphasizes the requirement of core proteins being assembled into capsids prior to interaction with LHBs.

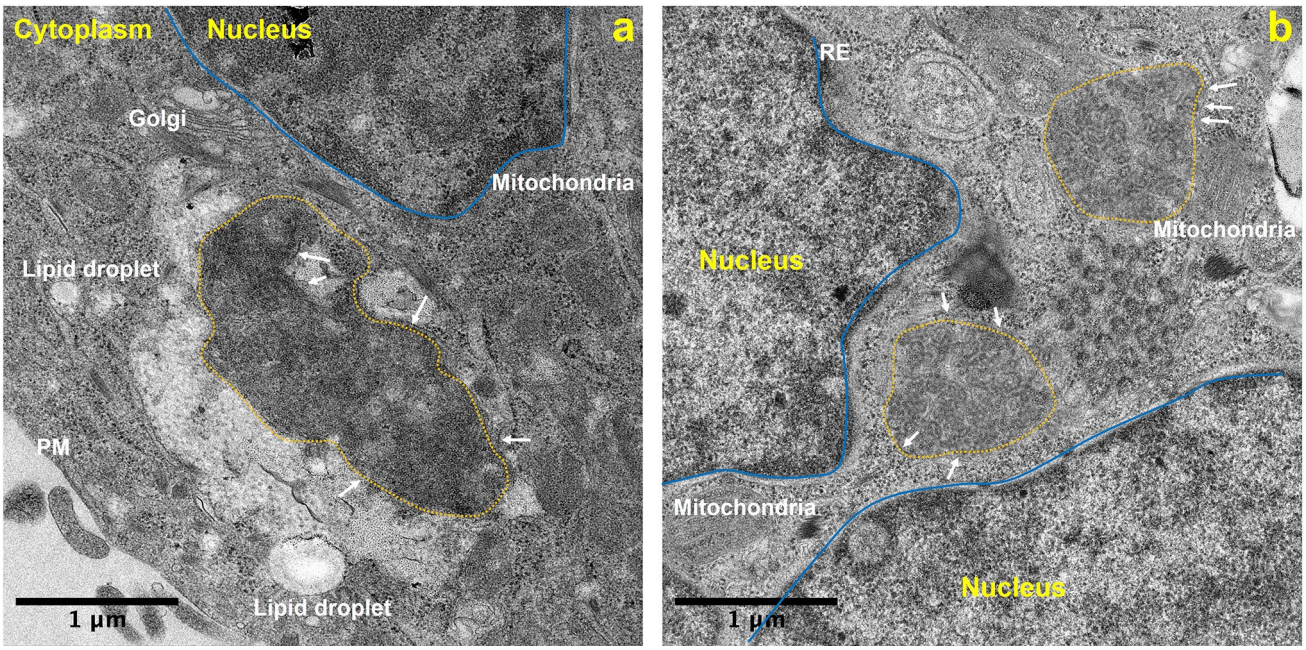

Fig. 4 LHBs mediates HBV capsids clustering in large cytoplasmic compartments observed by TEM. Huh-7 cells were transfected with a mixture of DNA plasmids expressing core, LHBs and eGFP-LHBs (50/45/5) for 72 h. The cells were sorted, fixed and ultrathin sections were cut and contrast-stained with uranyl acetate/citrate for regular transmission electron microscopy. Images a and b are two examples of large clusters of HBV capsids (orange dotted line) observed in intracellular compartments. White arrows indicate that HBV capsids accumulate within an intracellular compartment surrounded by a membrane. Some other cellular compartments or organelles are named in white. ER, Endoplasmic Reticulum and PM, Plasma Membrane

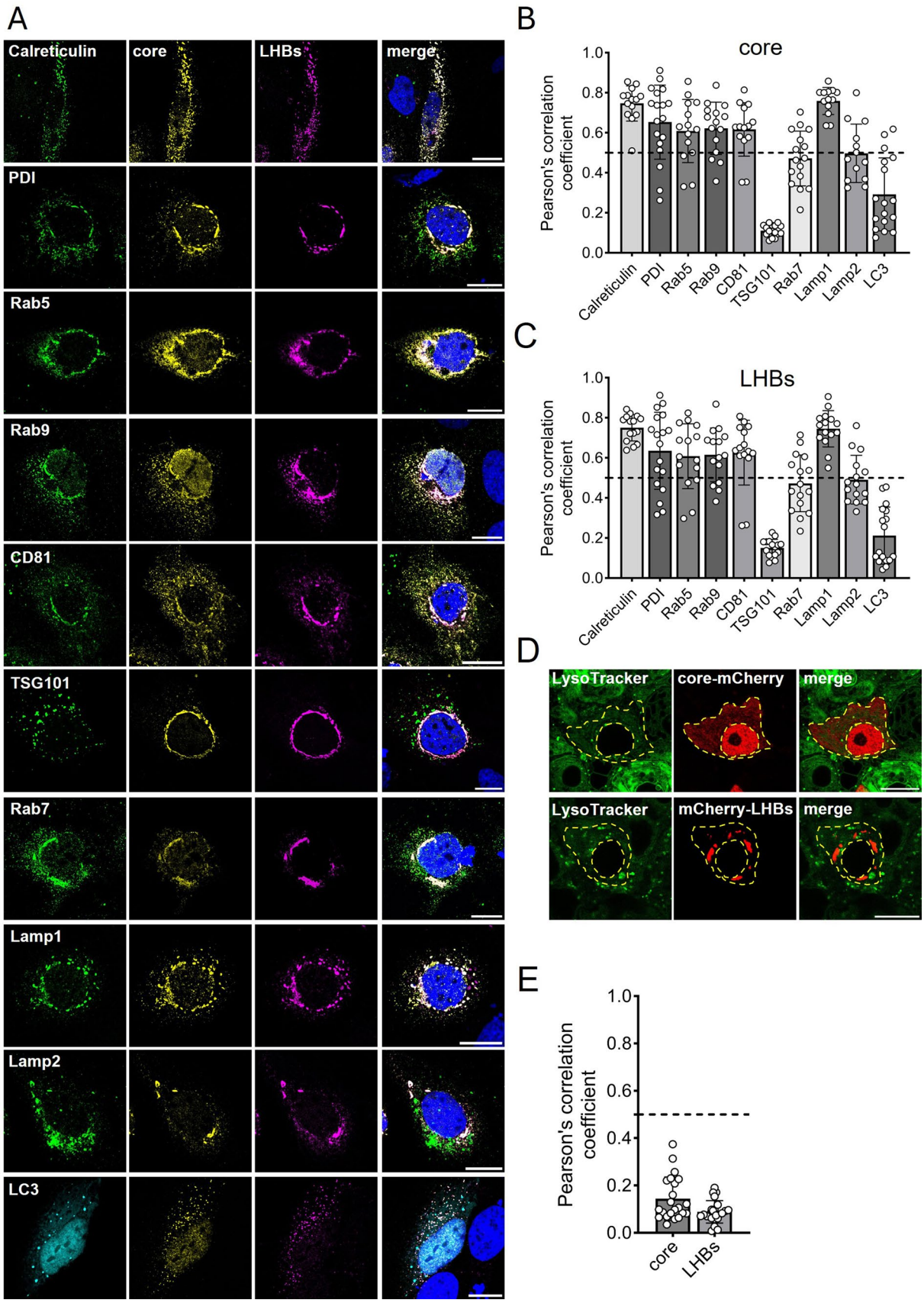
A
Calreticulin
core
LHBs
merge
PDI
Rab5
Rab9
CD81
TSG101
Rab7
Lamp1
Lamp2
LC3
B
core
Pearson's correlation coefficient
1.0
0.8
0.6
0.4
0.2
0.0
Calreticulin
PDI
Rab5
Rab9
CD81
TSG101
Rab7
Lamp1
Lamp2
LC3
C
LHBs
Pearson's correlation coefficient
D
LysoTracker
core-mCherry
merge
LysoTracker
mCherry-LHBs
merge
E
Pearson's correlation coefficient
core
LHBs

◂**Fig. 5** Co-localization of core-LHBs with markers of intracellular compartments. Huh-7 Cells were co-transfected with plasmids expressing core and LHBs. After 72 h, cells were fixed, permeabilized and immunostained. (A) In the green channel, images were obtained by immunofluorescence using anti-endosomal markers targeting endogenous proteins or using anti-HA for TSG101 or using aquamarine signal of LC3-Aquamarine protein in cyan. In yellow, the human anti-HBc polyclonal antibody targeting core, and in the magenta, the goat anti-HBs monoclonal antibody (Fitzgerald 70HG15) or rabbit anti-pre S1 R271 targeting LHBs protein. DAPI nuclear staining is shown in blue in the merge panel. The scale bars in white correspond to 10 µm. (B and C) The bar graphs show the mean values of the Pearson's correlation coefficient (PCC) from 15–20 cells. The PCC was calculated independently for the green (or cyan) and yellow channels (B), or the green (or cyan) and magenta channels (C) for each cell. (D) After 72 h, cells transfected with core/core-mCherry (90/10) plasmids, or LHBs/ mCherry-LHBs (95/5) plasmids were washed and incubated with green lysoTracker in Leibovitz's L-15 medium at 37 °C for 30 min. Images show the acidified vesicles staining in green, with core (upper panels) or LHBs (lower panels) in red. Cell periphery and nucleus are shown by orange dotted line. The scale bars in white correspond to 10 µm. (E) The mean values of the PCC of 20—25 cells are shown. In all cases scatter dots represent each cell analyzed from two independent experiments. The bars represent the mean values and the error bars the ± SD of the PCC. Representative images are shown

HBV capsids-LHBs complexes accumulate in large intracytoplasmic compartments

Immunogold labeling above described requires specific cell preparation, in particular lighter chemical fixation to preserve the antigenic properties of the proteins. As a result, this leads to lower contrast of acquired images and it is associated with less precise definition of cell structures. To precisely visualize the intracellular architecture of capsid-LHBs clusters, regular TEM was chosen because of its property to preserve the overall intra-cellular architecture. LHBs + eGFP-LHBs (95/5) + core proteins were co-expressed in Huh-7 cells and transfected cells were sorted for eGFP expression; selected cells were then prepared for TEM. Large electron-dense areas containing numerous intact capsid shells (orange dotted line), often close to the nucleus, were observed (Figs. 4a, b, S4). All capsids appeared in dense clusters as seen by immuno-TEM. Under these conditions, there was evidence of membrane-surrounded capsid clusters (white arrows in Figs. 4a, b, S4). Taken together, TEM and immuno-TEM observations highly favor the notion that HBV capsid-LHBs interactions are formed in intracellular compartments containing internal membranes.

HBV core-LHBs complexes localize in late endosomes/MVB

Given that our TEM images clearly show that the capsid-LHBs complex is associated with membranes, we next carried out experiments to further identify the intracellular compartment in which capsid-LHBs complexes are formed. We used markers of the endoplasmic reticulum (ER) (calreticulin, calnexin and PDI), early endosomes (Rab5), late endosomes/MVB (Rab7, Rab9, CD81, HA-TSG101) and late endosomes/lysosomes (Lamp 1 and Lamp 2) in cells co-expressing core and LHBs. Transfected cells were then imaged by confocal microscopy and the co-localization between the cellular markers (green) and core (yellow) and LHBs (magenta) was quantified by the Pearson correlation coefficient (Fig. 5B for core and Fig. 5C for LHBs). As shown in Fig. 5, there is a strong co-localization between calreticulin (or calnexin, not shown) and core and LHBs, with a R value of 0.75 ± 0.09 (first row). These two proteins are ubiquitous chaperone proteins that promote assembly and folding of proteins at the ER membrane [62]. ER is also the site of the HBV envelope proteins synthesis and oligomerization via multiple disulfide bounds [63–65], and PDI has been proposed to be involved in the assembly process [66]. To test this hypothesis, we performed a PDI-targeted IF and noted, in agreement with previous studies [27], an efficient co-localization of core-LHBs with PDI with a R value of 0.65 ± 0.2 (second row).

The knowledge of an intimate relationship between ER and endosomal pathway [67] prompted us to test other membrane markers. We confirmed endosomal localization of core-LHBs with Rab 5 and Rab 9 (R value ~ 0.60) (Fig. 5, third and fourth rows) [19, 68, 69]. The Rab family consists of small GTPases that serve as master regulators of membrane trafficking in eukaryotes and localizes from early to late endosomes/MVB [70]. In fact, we identified an efficient co-localization of core-LHBs complex and CD81 in cells co-expressing core and LHBs with a R value of 0.61 ± 0.1 (fifth row). CD81 belongs to the tetraspanin family and is a marker of late endosome and MVB. Interestingly, another marker of MBV, TSG101, was tested on cell co-transfected with core + LHBs + HA-TSG101 and no co-localization between core-LHBs and TSG101 was detected (sixth row). TSG101 also referred to as Vps23 protein is a subunit of ESCRT-I [71] belongs to membrane of exosomes [72] and is involved in membrane protein sorting that facilitates the final stages of virus release [73]. The absence of co-localization of core-LHBs complex with TSG101 could results from the lack of SHBs that is dramatic for virion egress [74].

As sorting occurs, endosomal subdomains mature and, ultimately, fuse with a degradative compartment named lysosome [75]. Nevertheless, the co-localization between core-LHBs complex and Rab 7 was less effective with R = 0.47 ± 0.14 (seventh row). This protein is a marker of late endosome maturation toward the degradation pathway of endocytosed cargos. In fact, lysosomes, and often autophagosomes, are associated with Rab7 effectors [76]. In

this context, we observed a strong co-localization between core-LHBs and endogenous Lamp1 with $R = 0.76 \pm 0.06$ (eighth row), but a lesser co-localization of membrane-cloaked capsids with Lamp 2 (ninth row, $R = 0.50 \pm 0.14$). In contrast, there was no co-localization of core or LHBs and the LysoTracker, with R values of 0.14 ± 0.09 and 0.27 ± 0.17 respectively (Fig. 5D, E). We could not show in addition evidence of core-LHBs being able to recruit the autophagy machinery [16] since core-LHBs and LC3 did not co-localize in cell expressing the viral proteins together with LC3-aquamarine ($R = 0.30 \pm 0.2$, tenth row in Fig. 5A).

Finally, the strong co-localization between core, LHBs and Lamp1 observed by confocal microscopy (eighth row) was confirmed by IF on cell expressing Lamp1-mTurquoise and LHBs (Fig. S5) and by immuno-TEM on cell expressing core + LHBs (Fig. 6). In this latter electron micrograph, capsids are identified by their shape, the smaller gold beads are targeting LHBs while the larger Lamp1. As aforementioned, capsids are clustered together with LHBs in the cytoplasm intimately associated with membranes expressing Lamp1 proteins.

All the experiments were also carried out on cells expressing LHBs alone (Fig. S6) and images, and Pearson coefficients, were very similar to those shown in Fig. 5. All together, these results show that LHBs drive core-LHBs clusters in the ER/endosomal pathway and their accumulation in neutral vesicles.

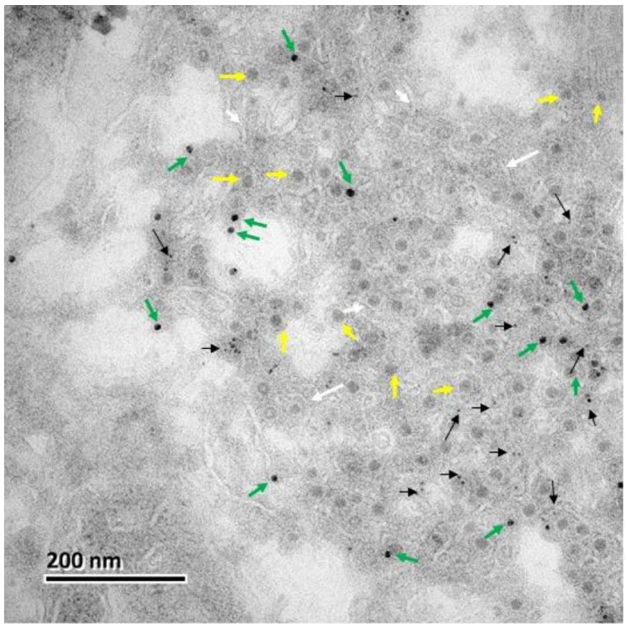

Fig. 6 Immuno-TEM of core-LHBs complexes and Lamp1. Huh-7 cells transfected with the mix of plasmids expressing core, LHBs and eGFP-LHBs (50/45/5) were sorted by FACS, centrifuged and the pellet treated for observation by immuno-TEM. Ultrathin sections were cut and incubated with a mouse anti-PreS1 M18/7 and rabbit anti-Lamp1 then with a 10-nm gold-conjugated anti-mouse antibody and with a 6-nm gold-conjugated anti-rabbit antibody. Scale is reported at the bottom left. Yellow arrows correspond to capsids, white arrows correspond to convoluted membranes, black arrows correspond to LHBs and green arrows correspond to Lamp1

Discussion

A major difficulty for documenting the morphogenesis of HBV virion—and the envelopment of the HBV nucleocapsid in particular -within a permissive cell by microscopy, lies with the fact that this essential step occurs in the cytoplasm together with numerous HBV SVPs including empty virions. It is therefore difficult to attribute a function to a viral protein. In addition, the HBV genome is highly condensed, making it difficult to insert fluorescent markers [77]. To follow HBV morphogenesis, we therefore chose to co-express the two main actors responsible for the critical stage of virion envelope acquisition, namely core and LHBs [8, 28, 30, 31]. In the absence of S, our model nevertheless does not provide a complete morphogenesis of the viral particle but has the merit of mimicking the early events of viral morphogenesis making them observable thanks to an accumulation of capsids associated with L-rich membranes [78, 79]. In addition, even though empty virions (devoid of HBV DNA) are usually produced at up 100-fold excess over complete virions [25] the morphogenesis events of complete virions and genome-free particles have been proposed to be similar [80].

In the context of LHBs and core co-expression large oligomers of LHBs proteins forming a crescent shape at the nuclear periphery as well as large dots dispersed within the cytoplasm were visualized by TEM (Figs. 3, 4). This self-oligomerization of LHBs was also observed by FLIM (Fig. S1) with a high FRET efficiency of 35% demonstrating a tight LHBs-LHBs interaction, but the resolution of the TEM clearly shows in addition that LHBs condensates in membrane-rich regions (Fig. 3, white arrows) [27, 35, 54]. These images of LHBs and core-LHBs clusters in membrane rich region are not due to an artifact of the Tokuyasu method. This method has long been presented as a method of choice for maintaining excellent cell morphology [58]. In fact, cells are frozen to obtain ultrathin sectioning and the structures remain fully hydrated throughout the labeling procedure to facilitate antibody interaction. Ultrastructures are also preserved by using mild fixing agents and glucose that avoid ice crystal formation which ensured an excellent morphology.

Finally, even if we consider that the confocal and FLIM images are limited by the resolution of the fluorescence microscope (250–300 nm), clusters obtained in TEM are in full agreement with observation of large clusters of proteins

on cells in Figs. 2, 5. It is important to underline that chimeric LHBs proteins were not myristoylated. However, LHBs myr(-) proteins are competent for virion assembly and secretion [47, 48], and LHBs association to the ER compartment is myristoylation-independent [79]. One cannot exclude that the N-terminally fused GFP (or mCherry) does indeed trap the preS1 domain in the cytosol and thereby favors the interaction between the latter and core. Nevertheless, eGFP- or mCherry-tagged myr(-) LHBs were always co-expressed with wt LHBs at 0.5/10 to 1/10 ratios, for FLIM or TEM respectively.

Regarding core, TEM of cell expressing wt core shows capsids alone with a regular electron-dense shape distributed within nucleus and cytoplasm (Fig. 4)[36, 45] in contrast with coreY132A that does not form capsids (Figs. 2, 3) which clearly shows an assembly defect observed by FLIM (Fig. S2). The absence of free core detection in the cell environment is consistent with the rapid kinetic of capsid assembly as previously reported [81]. Of note, the intracellular distribution of capsids would not depend on time of harvest since all experiments were performed at 72 h post-transfection [45].

While a few studies have shown the importance of core and LHBs for nucleocapsid envelopment, our data by FLIM demonstrates a direct interaction between core and LHBs that leads to core-LHBs complex in LHBs condensates (Fig. 2). It is remarkable that in cells co-expressing core and LHBs, the nucleus is partially emptied of core proteins; most of core proteins are sequestered as assembled capsids interacting with LHBs in membrane-rich region (Figs. 2, 3). As shown in Fig. 3 (images b-d), the localization of LHBs is not affected by the presence of capsids or its membrane environment, demonstrating that LHBs is responsible for recruiting capsids at membrane rich region to initiate virion envelopment.

Our approach to image HBV morphogenesis was reinforced by using two mutants described as essential for production of HBV virions. The capsid assembly-deficient coreY132A [55, 56] (Figs. 2, S2) was clearly deficient for interacting with LHBs, in support of our interpretation that preassembled capsid is the substrate for envelopment (Fig. 3). Similarly, deletion of MD in LHBs resulted in the lack of core-LHBs interaction as measured by FRET (Fig. 2), and of capsid-LHBs association as observed by TEM (Fig. 3) [28] but this MD deletion has no impact LHBs oligomerization (Fig. 1S). There is thus a requirement of capsid assembly for core-LHBs interaction. It will be interesting to combine the two microscopy approaches (quantitative fluorescent microscopy and TEM) to test the interaction between LHBs and core mutated in the linker domain (aas 140–150) that has been reported not to impact capsid formation (in presence of CTD) but to severely impair empty virions secretion, suggesting a defect for capsid-LHBs interaction that could be independent from capsid assembly [82]. It is similarly crucial to investigate the effects of mutations in the core-CTD on the interaction between LHBs and capsid. Previous studies have indicated that mutations or deletions in the core-CTD can hinder core assembly, possibly due to the interaction of this highly basic peptide with nucleic acids, which facilitates core self-assembly [36, 83–85].

In agreement with previous reports [7, 35, 60, 86], our study also shows that empty capsids do not interact directly with the SHBs (Fig. 2). Even though the cytosolic loop of SHBs was reported to include a potential capsid-binding domain (aa 56 ± 80) [33, 34], we have not detected any intracellular interaction between SHBs and core [32, 87]. Such an interaction was reported in vitro to be of low affinity (> 80 µM) [88], which may not be detectable by FLIM in cellular context.

Capsid-LHBs complex localizes at the periphery of the nucleus in a region that carries ER markers [15, 89] such as calnexin and calreticulin, chaperon proteins, which together with Hsc70 and BiP were shown important for the proper topology of LHBs at the ER membrane [90, 91]. Core-LHBs complexes in addition co-localize with several markers such as Lamp 1, Rab 5, 9 and CD81, suggesting that capsid envelopment would occur in early (Rab 5) to late (Rab 9) endosomes, including MVBs (CD81). Note that Rab5 is important to drive the translocation of LHBs from ER to MVBs in the presence of SHBs [69] but we show here that the sole expression of LHBs is sufficient for capsid-LHBs to accumulate in Rab5 positive endosomes reinforcing the importance of LHBs in driving capsid envelopment. In fact, the localization of the capsid-LHBs complexes in endosome/MVB is similar to that of LHBs in the absence of core (compare Figs. 5, S6) in agreement with LHBs building the platform for assembly [26, 27, 35].

Co-localization of capsid-LHBs and Lamp1 is also an indication for the involvement of late endosomes. In HepG2.2.15 cells, or HBV DNA-transfected Huh-7 cells, a co-localization of viral particles with Lamp1 has already been observed. Here we show that LHBs is the driving force to this particular compartment [18, 26]. Lamp1 is also a lysosome marker, but we observed only a limited co-localization of core-LHBs with Rab7, and no co-localization with lamp 2 and the LysoTracker, suggesting that the core-LHBs complex is not in an acidic environment.

Interestingly, we did not find any co-localization of core-LHBs and TSG101, consistent with the fact that TGS101 is not differently distributed in a HBV positive (HepG2.2.15) and negative (HepG2) cells [26]. In fact, TSG101 was shown dispensable for HBV egress [92] and neither core, nor LHBs, contains a P(S/T)AP late motif domain [93]. However, TSG101 belongs to the ESCRT1 family of proteins and is essential for HBV secretion via the MVB pathway by direct

recruitment of the ubiquitinylated core protein [22] or via α-taxalin acting as a linker between the envelope proteins and TSG101 [94]. The absence of SHBs in our experimental model, which consequently prevents particles secretion, could explain the absence of correlation between core-LHBs and TSG101 in this study.

Although autophagosome membranes have been described as important for nucleocapsid assembly and virion release [95], such structures, usually identified as double-membrane vesicles [96] could not be observed in our TEM images. Furthermore, our IF experiments did not reveal any co-localization of LC3, Rab7 with core or LHBs (Fig. 5). This result could be explained by the absence of the HBx, SHBs or HBe previously reported as responsible for the induction of autophagy [18, 20, 26].

In conclusion, we have shown that the envelopment of HBV capsid prior to HBV virion release, is essentially orchestrated by LHBs that condenses large amount of pre-assembled capsid in ER-derived membranes of the endosomal pathway, but not related to acidic vesicles nor to autophagosomes.

Acknowledgements This is work was supported by the Agence Nationale de Recherche sur le SIDA et les hépatites virales (ANRS-MIE, https://anrs.fr/fr/) and by La Ligue contre le cancer (https://www.ligue-cancer.net/). We thank Jean-Luc Darlix for fruitful discussion. We also thank Juliette Rousseau and all the members of the Electron Microscopy platform (IBiSA) of Tours University (http://microscopies.med.univ-tours.fr) for technical support. We thank Lena Sintes for coloring the viruses. We thank the Plateforme B Cell Ressources, EA4245 Facility of Tours University for technical support, Addgene for pLamp1-mTurquoise2, Dr Laurence Cocquerel for anti-CD81 and Giulia Bertolin for pAquamarin-LC3B.

Author contributions Florian Seigneuret and Sébastien Eymieux carried out most of the electron microscopy experiments, Julien Burlaud-Gaillard and Pierre Raynal oversee the microscopy platform, Vanessa Sarabia-Vega and Roxane Lemoine are in charge of cell biology, cell sorting, and Christophe Hourioux, Philippe Roingeard, Camille Sureau and Hugues de Rocquigny took part in analyzing images, and data, writing the manuscript and seeking funding. All authors read and approved the final manuscript.

Funding This work was funded by Institut National de la Sante et de la Recherche Medicale (INSERM) and University of Tours. The funders had no role in study design, data collection and analysis, decision to publish, or preparation of the manuscript. It was also supported by Agence Nationale de Recherche sur le Sida et les hepatites virales (ANRS-MIE) with a grant for Vanessa Sarabia-Vega (ECTZ 225768), and La Ligue, (AO 2021).

Data availability The data that support the findings of this study are available on request from the corresponding author.

Declarations

Conflict of interest The authors have declared that no competing interests exist.

Ethical approval Not applicable.

Consent for publication Not applicable.

References

1. Inoue J, Sato K, Ninomiya M, Masamune A (2021) Envelope proteins of hepatitis B virus: molecular biology and involvement in carcinogenesis. Viruses. https://doi.org/10.3390/v13061124
2. Huovila AP, Eder AM, Fuller SD (1992) Hepatitis B surface antigen assembles in a post-ER, pre-Golgi compartment. J Cell Biol 118:1305–1320. https://doi.org/10.1083/jcb.118.6.1305
3. Patient R, Hourioux C, Roingeard P (2009) Morphogenesis of hepatitis B virus and its subviral envelope particles. Cell Microbiol 11:1561–1570. https://doi.org/10.1111/j.1462-5822.2009.01363.x
4. Fernholz D, Stemler M, Brunetto M, Bonino F, Will H (1991) Replicating and virion secreting hepatitis B mutant virus unable to produce preS2 protein. J Hepatol 13(4):S102–S104. https://doi.org/10.1016/0168-8278(91)90036-b
5. Santantonio T, Jung MC, Schneider R, Fernholz D, Milella M, Monno L, Pastore G, Pape GR, Will H (1992) Hepatitis B virus genomes that cannot synthesize pre-S2 proteins occur frequently and as dominant virus populations in chronic carriers in Italy. Virology 188:948–952. https://doi.org/10.1016/0042-6822(92)90559-8
6. Fernholz D, Galle PR, Stemler M, Brunetto M, Bonino F, Will H (1993) Infectious hepatitis B virus variant defective in pre-S2 protein expression in a chronic carrier. Virology 194:137–148. https://doi.org/10.1006/viro.1993.1243
7. Le Seyec J, Chouteau P, Cannie I, Guguen-Guillouzo C, Gripon P (1999) Infection process of the hepatitis B virus depends on the presence of a defined sequence in the pre-S1 domain. J Virol 73:2052–2057. https://doi.org/10.1128/JVI.73.3.2052-2057.1999
8. Bruss V, Ganem D (1991) The role of envelope proteins in hepatitis B virus assembly. Proc Natl Acad Sci U S A 88:1059–1063. https://doi.org/10.1073/pnas.88.3.1059
9. Prange R (2022) Hepatitis B virus movement through the hepatocyte: an update. Biol Cell 114:325–348. https://doi.org/10.1111/boc.202200060
10. Liu H, Zakrzewicz D, Nosol K, Irobalieva RN, Mukherjee S, Bang-Sorensen R, Goldmann N, Kunz S, Rossi L, Kossiakoff AA, Urban S, Glebe D, Geyer J, Locher KP (2024) Structure of antiviral drug bulevirtide bound to hepatitis B and D virus receptor protein NTCP. Nat Commun 15:2476. https://doi.org/10.1038/s41467-024-46706-w
11. Yan H, Zhong G, Xu G, He W, Jing Z, Gao Z, Huang Y, Qi Y, Peng B, Wang H, Fu L, Song M, Chen P, Gao W, Ren B, Sun Y, Cai T, Feng X, Sui J, Li W (2012) Sodium taurocholate

cotransporting polypeptide is a functional receptor for human hepatitis B and D virus. Elife 1:e00049. https://doi.org/10.7554/eLife.00049
12. Hirsch RC, Lavine JE, Chang LJ, Varmus HE, Ganem D (1990) Polymerase gene products of hepatitis B viruses are required for genomic RNA packaging as wel as for reverse transcription. Nature 344:552–555. https://doi.org/10.1038/344552a0
13. Bruss V (2007) Hepatitis B virus morphogenesis. World J Gastroenterol 13:65–73. https://doi.org/10.3748/wjg.v13.i1.65
14. Seeger C, Mason WS (2015) Molecular biology of hepatitis B virus infection. Virology 479–480:672–686. https://doi.org/10.1016/j.virol.2015.02.031
15. Xu Z, Bruss V, Yen TS (1997) Formation of intracellular particles by hepatitis B virus large surface protein. J Virol 71:5487–5494. https://doi.org/10.1128/jvi.71.7.5487-5494.1997
16. Dreux M, Chisari FV (2010) Viruses and the autophagy machinery. Cell Cycle 9:1295–1307. https://doi.org/10.4161/cc.9.7.11109
17. Doring T, Zeyen L, Bartusch C, Prange R (2018) Hepatitis B virus subverts the autophagy elongation complex Atg5–12/16L1 and does not require Atg8/LC3 lipidation for viral maturation. J Virol. https://doi.org/10.1128/JVI.01513-17
18. Sir D, Tian Y, Chen WL, Ann DK, Yen TS, Ou JH (2010) The early autophagic pathway is activated by hepatitis B virus and required for viral DNA replication. Proc Natl Acad Sci U S A 107:4383–4388. https://doi.org/10.1073/pnas.0911373107
19. Cui S, Xia T, Zhao J, Ren X, Wu T, Kameni M, Guo X, He L, Guo J, Duperray-Susini A, Levillayer F, Collard JM, Zhong J, Pan L, Tangy F, Vidalain PO, Zhou D, Jiu Y, Faure M, Wei Y (2023) NDP52 mediates an antiviral response to hepatitis B virus infection through Rab9-dependent lysosomal degradation pathway. Nat Commun 14:8440. https://doi.org/10.1038/s41467-023-44201-2
20. Li J, Liu Y, Wang Z, Liu K, Wang Y, Liu J, Ding H, Yuan Z (2011) Subversion of cellular autophagy machinery by hepatitis B virus for viral envelopment. J Virol 85:6319–6333. https://doi.org/10.1128/jvi.02627-10
21. Lin Y, Zhao Z, Huang A, Lu M (2020) Interplay between cellular autophagy and hepatitis B virus replication: a systematic review. Cells. https://doi.org/10.3390/cells9092101
22. Zheng Y, Wang M, Li S, Bu Y, Xu Z, Zhu G, Wu C, Zhao K, Li A, Chen Q, Wang J, Hua R, Teng Y, Zhao L, Cheng X, Xia Y (2023) Hepatitis B virus hijacks TSG101 to facilitate egress via multiple vesicle bodies. PLoS Pathog 19:e1011382. https://doi.org/10.1371/journal.ppat.1011382
23. Rost M, Mann S, Lambert C, Doring T, Thome N, Prange R (2006) Gamma-adaptin, a novel ubiquitin-interacting adaptor, and Nedd4 ubiquitin ligase control hepatitis B virus maturation. J Biol Chem 281:29297–29308. https://doi.org/10.1074/jbc.M603517200
24. Hu J, Liu K (2017) Complete and incomplete hepatitis B virus particles: formation, function, and application. Viruses. https://doi.org/10.3390/v9030056
25. Ning X, Nguyen D, Mentzer L, Adams C, Lee H, Ashley R, Hafenstein S, Hu J (2011) Secretion of genome-free hepatitis B virus–single strand blocking model for virion morphogenesis of para-retrovirus. PLoS Pathog 7:e1002255. https://doi.org/10.1371/journal.ppat.1002255
26. Inoue J, Krueger EW, Chen J, Cao H, Ninomiya M, McNiven MA (2015) HBV secretion is regulated through the activation of endocytic and autophagic compartments mediated by Rab7 stimulation. J Cell Sci 128:1696–1706. https://doi.org/10.1242/jcs.158097
27. Jiang B, Himmelsbach K, Ren H, Boller K, Hildt E (2015) Subviral hepatitis B virus filaments, like infectious viral particles, are released via multivesicular bodies. J Virol 90:3330–3341. https://doi.org/10.1128/jvi.03109-15
28. Bruss V (1997) A short linear sequence in the pre-S domain of the large hepatitis B virus envelope protein required for virion formation. J Virol 71:9350–9357. https://doi.org/10.1128/JVI.71.12.9350-9357.1997
29. Bruss V (2004) Envelopment of the hepatitis B virus nucleocapsid. Virus Res 106:199–209. https://doi.org/10.1016/j.virusres.2004.08.016
30. Summers J, Smith PM, Horwich AL (1990) Hepadnavirus envelope proteins regulate covalently closed circular DNA amplification. J Virol 64:2819–2824. https://doi.org/10.1128/JVI.64.6.2819-2824.1990
31. Summers J, Smith PM, Huang MJ, Yu MS (1991) Morphogenetic and regulatory effects of mutations in the envelope proteins of an avian hepadnavirus. J Virol 65:1310–1317. https://doi.org/10.1128/JVI.65.3.1310-1317.1991
32. Ning X, Luckenbaugh L, Liu K, Bruss V, Sureau C, Hu J (2018) Common and distinct capsid and surface protein requirements for secretion of complete and genome-free hepatitis B virions. J Virol. https://doi.org/10.1128/jvi.00272-18
33. Hourioux C, Touze A, Coursaget P, Roingeard P (2000) DNA-containing and empty hepatitis B virus core particles bind similarly to envelope protein domains. J Gen Virol 81:1099–1101. https://doi.org/10.1099/0022-1317-81-4-1099
34. Poisson F, Severac A, Hourioux C, Goudeau A, Roingeard P (1997) Both pre-S1 and S domains of hepatitis B virus envelope proteins interact with the core particle. Virology 228:115–120. https://doi.org/10.1006/viro.1996.8367
35. Pastor F, Herrscher C, Patient R, Eymieux S, Moreau A, Burlaud-Gaillard J, Seigneuret F, de Rocquigny H, Roingeard P, Hourioux C (2019) Direct interaction between the hepatitis B virus core and envelope proteins analyzed in a cellular context. Sci Rep 9:16178. https://doi.org/10.1038/s41598-019-52824-z
36. Rat V, Pinson X, Seigneuret F, Durand S, Herrscher C, Lemoine R, Burlaud-Gaillard J, Raynal PY, Hourioux C, Roingeard P, Tramier M, de Rocquigny H (2020) Hepatitis B virus core protein domains essential for viral capsid assembly in a cellular context. J Mol Biol. https://doi.org/10.1016/j.jmb.2020.04.026
37. Nakabayashi H, Taketa K, Miyano K, Yamane T, Sato J (1982) Growth of human hepatoma cells lines with differentiated functions in chemically defined medium. Cancer Res 42:3858–3863
38. Yaginuma K, Shirakata Y, Kobayashi M, Koike K (1987) Hepatitis B virus (HBV) particles are produced in a cell culture system by transient expression of transfected HBV DNA. Proc Natl Acad Sci U S A 84:2678–2682. https://doi.org/10.1073/pnas.84.9.2678
39. Roingeard P, Lu SL, Sureau C, Freschlin M, Arbeille B, Essex M, Romet-Lemonne JL (1990) Immunocytochemical and electron microscopic study of hepatitis B virus antigen and complete particle production in hepatitis B virus DNA transfected HepG2 cells. Hepatology 11:277–285
40. Bentaleb C, Hervouet K, Montpellier C, Camuzet C, Ferrie M, Burlaud-Gaillard J, Bressanelli S, Metzger K, Werkmeister E, Ankavay M, Janampa NL, Marlet J, Roux J, Deffaud C, Goffard A, Rouille Y, Dubuisson J, Roingeard P, Alioua-Denis CM, Cocquerel L (2022) The endocytic recycling compartment serves as a viral factory for hepatitis E virus. Cell Mol Life Sci 79:615. https://doi.org/10.1007/s00018-022-04646-y
41. Julithe R, Abou-Jaoude G, Sureau C (2014) Modification of the hepatitis B virus envelope protein glycosylation pattern interferes with secretion of viral particles, infectivity, and susceptibility to neutralizing antibodies. J Virol 88:9049–9059. https://doi.org/10.1128/JVI.01161-14
42. Gokerkucuk EB, Cheron A, Tramier M, Bertolin G (2023) The LC3B FRET biosensor monitors the modes of action of ATG4B during autophagy in living cells. Autophagy 19:2275–2295. https://doi.org/10.1080/15548627.2023.2179845

43. El Meshri SE, Boutant E, Mouhand A, Thomas A, Larue V, Richert L, Vivet-Boudou V, Mely Y, Tisne C, Muriaux D, de Rocquigny H (2018) The NC domain of HIV-1 Gag contributes to the interaction of Gag with TSG101. Biochim Biophys Acta Gen Subj 1862:1421–1431. https://doi.org/10.1016/j.bbagen.2018.03.020
44. Yeh CT, Ou JH, Chu CM, Liaw YF (1994) Alteration of the subcellular localization of hepatitis B virus core protein by large but not small surface proteins. Biochem Biophys Res Commun 203:1348–1354. https://doi.org/10.1006/bbrc.1994.2330
45. Romero S, Unchwaniwala N, Evans EL 3rd, Eliceiri KW, Loeb DD, Sherer NM (2023) Live cell imaging reveals HBV capsid translocation from the nucleus to the cytoplasm enabled by cell division. mBio 14:e0330322. https://doi.org/10.1128/mbio.03303-22
46. Kratz PA, Bottcher B, Nassal M (1999) Native display of complete foreign protein domains on the surface of hepatitis B virus capsids. Proc Natl Acad Sci U S A 96:1915–1920
47. Gripon P, Le Seyec J, Rumin S, Guguen-Guillouzo C (1995) Myristylation of the hepatitis B virus large surface protein is essential for viral infectivity. Virology 213:292–299. https://doi.org/10.1006/viro.1995.0002
48. Bruss V, Hagelstein J, Gerhardt E, Galle PR (1996) Myristylation of the large surface protein is required for hepatitis B virus in vitro infectivity. Virology 218:396–399. https://doi.org/10.1006/viro.1996.0209
49. de Rocquigny H, El Meshri SE, Richert L, Didier P, Darlix JL, Mely Y (2014) Role of the nucleocapsid region in HIV-1 Gag assembly as investigated by quantitative fluorescence-based microscopy. Virus Res 193:78–88. https://doi.org/10.1016/j.virusres.2014.06.009
50. Richert L, Didier P, de Rocquigny H, Mély Y (2015) Monitoring HIV-1 protein oligomerization by FLIM FRET Microscopy. Adv Time-Correlated Single Photon Counting Appl 111:277–307
51. Bastiaens PI, Squire A (1999) Fluorescence lifetime imaging microscopy: spatial resolution of biochemical processes in the cell. Trends Cell Biol 9:48–52. https://doi.org/10.1016/s0962-8924(98)01410-x
52. Voss TC, Demarco IA, Day RN (2005) Quantitative imaging of protein interactions in the cell nucleus. Biotechniques 38:413–424. https://doi.org/10.2144/05383RV01
53. Tramier M, Zahid M, Mevel JC, Masse MJ, Coppey-Moisan M (2006) Sensitivity of CFP/YFP and GFP/mCherry pairs to donor photobleaching on FRET determination by fluorescence lifetime imaging microscopy in living cells. Microsc Res Tech 69:933–939. https://doi.org/10.1002/jemt.20370
54. Deroubaix A, Osseman Q, Cassany A, Begu D, Rages J, Kassab S, Laine S, Kann M (2015) Expression of viral polymerase and phosphorylation of core protein determine core and capsid localization of the human hepatitis B virus. J Gen Virol 96:183–195. https://doi.org/10.1099/vir.0.064816-0
55. Bourne CR, Katen SP, Fulz MR, Packianathan C, Zlotnick A (2009) A mutant hepatitis B virus core protein mimics inhibitors of icosahedral capsid self-assembly. Biochemistry 48:1736–1742. https://doi.org/10.1021/bi801814y
56. Klumpp K, Lam AM, Lukacs C, Vogel R, Ren S, Espiritu C, Baydo R, Atkins K, Abendroth J, Liao G, Efimov A, Hartman G, Flores OA (2015) High-resolution crystal structure of a hepatitis B virus replication inhibitor bound to the viral core protein. Proc Natl Acad Sci U S A 112:15196–15201. https://doi.org/10.1073/pnas.1513803112
57. Suffner S, Gerstenberg N, Patra M, Ruibal P, Orabi A, Schindler M, Bruss V (2018) Domains of the hepatitis B virus small surface protein S mediating oligomerization. J Virol. https://doi.org/10.1128/JVI.02232-17
58. Griffiths G, Slot JW, Webster P (2015) Kiyoteru Tokuyasu: a pioneer of cryo-ultramicrotomy. J Microsc 260:235–237. https://doi.org/10.1111/jmi.12346
59. Sumner C, Ono A (2022) Relationship between HIV-1 Gag multimerization and membrane binding. Viruses. https://doi.org/10.3390/v14030622
60. Le Seyec J, Chouteau P, Cannie I, Guguen-Guillouzo C, Gripon P (1998) Role of the pre-S2 domain of the large envelope protein in hepatitis B virus assembly and infectivity. J Virol 72:5573–5578. https://doi.org/10.1128/jvi.72.7.5573-5578.1998
61. Le Pogam S, Shih C (2002) Influence of a putative intermolecular interaction between core and the pre-S1 domain of the large envelope protein on hepatitis B virus secretion. J Virol 76:6510–6517. https://doi.org/10.1128/jvi.76.13.6510-6517.2002
62. Kohli E, Causse S, Baverel V, Dubrez L, Borges-Bonan N, Demidov O, Garrido C (2021) Endoplasmic reticulum chaperones in viral infection: therapeutic perspectives. Microbiol Mol Biol Rev 85:e0003521. https://doi.org/10.1128/MMBR.00035-21
63. Mangold CM, Unckell F, Werr M, Streeck RE (1995) Secretion and antigenicity of hepatitis B virus small envelope proteins lacking cysteines in the major antigenic region. Virology 211:535–543. https://doi.org/10.1006/viro.1995.1435
64. Nassal M, Rieger A, Steinau O (1992) Topological analysis of the hepatitis B virus core particle by cysteine-cysteine cross-linking. J Mol Biol 225:1013–1025. https://doi.org/10.1016/0022-2836(92)90101-o
65. Abou-Jaoudé G, Sureau C (2007) Entry of hepatitis delta virus requires the conserved cysteine residues of the hepatitis B virus envelope protein antigenic loop and is blocked by inhibitors of thiol-disulfide exchange. J Virol 81:13057–13066. https://doi.org/10.1128/jvi.01495-07
66. Perez-Vargas J, Teppa E, Amirache F, Boson B, Pereira de Oliveira R, Combet C, Bockmann A, Fusil F, Freitas N, Carbone A, Cosset FL (2021) A fusion peptide in preS1 and the human protein disulfide isomerase ERp57 are involved in hepatitis B virus membrane fusion process. Elife. https://doi.org/10.7554/eLife.64507
67. Di Mattia T, Tomasetto C, Alpy F (2020) Faraway, so close! Functions of endoplasmic reticulum-endosome contacts. Biochim Biophys Acta Mol Cell Biol Lipids 1865:158490. https://doi.org/10.1016/j.bbalip.2019.06.016
68. Macovei A, Petrareanu C, Lazar C, Florian P, Branza-Nichita N (2013) Regulation of hepatitis B virus infection by Rab5, Rab7, and the endolysosomal compartment. J Virol 87:6415–6427. https://doi.org/10.1128/jvi.00393-13
69. Inoue J, Ninomiya M, Umetsu T, Nakamura T, Kogure T, Kakazu E, Iwata T, Takai S, Sano A, Fukuda M, Watashi K, Isogawa M, Tanaka Y, Shimosegawa T, McNiven MA, Masamune A (2019) Small interfering RNA screening for the small GTPase Rab proteins identifies Rab5B as a major regulator of hepatitis B virus production. J Virol. https://doi.org/10.1128/JVI.00621-19
70. Kuchitsu Y, Fukuda M (2018) Revisiting Rab7 functions in mammalian autophagy: Rab7 knockout studies. Cells. https://doi.org/10.3390/cells7110215
71. Slagsvold T, Pattni K, Malerod L, Stenmark H (2006) Endosomal and non-endosomal functions of ESCRT proteins. Trends Cell Biol 16:317–326. https://doi.org/10.1016/j.tcb.2006.04.004

72. Gurung S, Perocheau D, Touramanidou L, Baruteau J (2021) The exosome journey: from biogenesis to uptake and intracellular signalling. Cell Commun Signal 19:47. https://doi.org/10.1186/s12964-021-00730-1
73. Votteler J, Sundquist WI (2013) Virus budding and the ESCRT pathway. Cell Host Microbe 14:232–241. https://doi.org/10.1016/j.chom.2013.08.012
74. Blondot ML, Bruss V, Kann M (2016) Intracellular transport and egress of hepatitis B virus. J Hepatol 64:S49–S59. https://doi.org/10.1016/j.jhep.2016.02.008
75. Jean S, Nassari S (2022) Regulation of endosomal sorting and maturation by ER-endosome contact sites. Contact (Thousand Oaks) 5:25152564221106050. https://doi.org/10.1177/25152564221106046
76. Poteryaev D, Datta S, Ackema K, Zerial M, Spang A (2010) Identification of the switch in early-to-late endosome transition. Cell 141:497–508. https://doi.org/10.1016/j.cell.2010.03.011
77. Zhang Z, Zehnder B, Damrau C, Urban S (2016) Visualization of hepatitis B virus entry - novel tools and approaches to directly follow virus entry into hepatocytes. FEBS Lett 590:1915–1926. https://doi.org/10.1002/1873-3468.12202
78. Chisari FV, Filippi P, Buras J, McLachlan A, Popper H, Pinkert CA, Palmiter RD, Brinster RL (1987) Structural and pathological effects of synthesis of hepatitis B virus large envelope polypeptide in transgenic mice. Proc Natl Acad Sci U S A 84:6909–6913. https://doi.org/10.1073/pnas.84.19.6909
79. Kuroki K, Russnak R, Ganem D (1989) Novel N-terminal amino acid sequence required for retention of a hepatitis B virus glycoprotein in the endoplasmic reticulum. Mol Cell Biol 9:4459–4466. https://doi.org/10.1128/mcb.9.10.4459-4466.1989
80. Liu K, Hu J (2019) Secretion of empty or complete hepatitis B virions: envelopment of empty capsids versus mature nucleocapsids. Futur Virol 14:95–105. https://doi.org/10.2217/fvl-2018-0128
81. Zlotnick A, Venkatakrishnan B, Tan Z, Lewellyn E, Turner W, Francis S (2015) Core protein: a pleiotropic keystone in the HBV lifecycle. Antiviral Res 121:82–93. https://doi.org/10.1016/j.antiviral.2015.06.020
82. Liu K, Luckenbaugh L, Ning X, Xi J, Hu J (2018) Multiple roles of core protein linker in hepatitis B virus replication. PLoS Pathog 14:e1007085. https://doi.org/10.1371/journal.ppat.1007085
83. Ludgate L, Liu K, Luckenbaugh L, Streck N, Eng S, Voitenleitner C, Delaney WEt and Hu J, (2016) Cell-free hepatitis B virus capsid assembly dependent on the core protein C-terminal domain and regulated by phosphorylation. J Virol 90:5830–5844. https://doi.org/10.1128/JVI.00394-16
84. Chu TH, Liou AT, Su PY, Wu HN, Shih C (2014) Nucleic acid chaperone activity associated with the arginine-rich domain of human hepatitis B virus core protein. J Virol 88:2530–2543. https://doi.org/10.1128/JVI.03235-13
85. de Rocquigny H, Rat V, Pastor F, Darlix JL, Hourioux C, Roingeard P (2020) Phosphorylation of the arginine-rich C-terminal domains of the hepatitis B virus (HBV) core protein as a fine regulator of the interaction between HBc and nucleic acid. Viruses. https://doi.org/10.3390/v12070738
86. Bruss V, Thomssen R (1994) Mapping a region of the large envelope protein required for hepatitis B virion maturation. J Virol 68:1643–1650. https://doi.org/10.1128/JVI.68.3.1643-1650.1994
87. Blanchet M, Sureau C (2006) Analysis of the cytosolic domains of the hepatitis B virus envelope proteins for their function in viral particle assembly and infectivity. J Virol 80:11935–11945. https://doi.org/10.1128/jvi.00621-06
88. Tan WS, Dyson MR, Murray K (1999) Two distinct segments of the hepatitis B virus surface antigen contribute synergistically to its association with the viral core particles. J Mol Biol 286:797–808. https://doi.org/10.1006/jmbi.1998.2525
89. Patzer EJ, Nakamura GR, Simonsen CC, Levinson AD, Brands R (1986) Intracellular assembly and packaging of hepatitis B surface antigen particles occur in the endoplasmic reticulum. J Virol 58:884–892. https://doi.org/10.1128/JVI.58.3.884-892.1986
90. Prange R, Werr M, Loffler-Mary H (1999) Chaperones involved in hepatitis B virus morphogenesis. Biol Chem 380:305–314. https://doi.org/10.1515/BC.1999.042
91. Lambert C, Prange R (2003) Chaperone action in the posttranslational topological reorientation of the hepatitis B virus large envelope protein: implications for translocational regulation. Proc Natl Acad Sci U S A 100:5199–5204. https://doi.org/10.1073/pnas.0930813100
92. Stieler JT, Prange R (2014) Involvement of ESCRT-II in hepatitis B virus morphogenesis. PLoS ONE 9:e91279. https://doi.org/10.1371/journal.pone.0091279
93. Rose KM, Hirsch VM, Bouamr F (2020) Budding of a retrovirus: some assemblies required. Viruses. https://doi.org/10.3390/v12101188
94. Hoffmann J, Boehm C, Himmelsbach K, Donnerhak C, Roettger H, Weiss TS, Ploen D, Hildt E (2013) Identification of alpha-taxilin as an essential factor for the life cycle of hepatitis B virus. J Hepatol 59:934–941. https://doi.org/10.1016/j.jhep.2013.06.020
95. Chu JYK, Chuang YC, Tsai KN, Pantuso J, Ishida Y, Saito T, Ou JJ (2022) Autophagic membranes participate in hepatitis B virus nucleocapsid assembly, precore and core protein trafficking, and viral release. Proc Natl Acad Sci U S A 119:e2201927119. https://doi.org/10.1073/pnas.2201927119
96. Eskelinen EL, Reggiori F, Baba M, Kovacs AL, Seglen PO (2011) Seeing is believing: the impact of electron microscopy on autophagy research. Autophagy 7:935–956. https://doi.org/10.4161/auto.7.9.15760